From biorefineries to bioproducts: conversion of pretreated pulp from biorefining streams to lignocellulose nanofibers

CHENGGUI SUN, YANG GAO, RICHARD CHANDRA, AND YAMAN BOLUK

ABSTRACT: This study investigates the use of pretreatment and enzymatic hydrolysis side streams and conversion to lignocellulose nanofibers. We used a steam-exploded and partial enzymatic hydrolyzed hardwood pulp and an organosolv pretreated softwood pulp to prepare lignocellulose nanofibers (LCNF) via microfluidization. The energies applied on fibrillation were estimated to examine the energy consumption levels of LCNF production. The energy consumptions of the fibrillation processes of the hardwood LCNF production and the softwood LCNF production were about 7040-14080 kWh/ton and 4640 kWh/ton on a dry material basis, respectively. The morphology and dimension of developed hardwood and softwood LCNFs and the stability and rheological behavior of their suspensions were investigated and are discussed.

Application: The development of LCNF as a high value coproduct from lignocellulosic biomass from side streams of biorefining processes could increase the economic feasibility of biorefining processes.

Lignocellulose nanofibers (LCNF) are sustainable and environmentally friendly bioproducts that can be prepared from cellulosic feedstocks, such as wood [1-5], wheat straw [6,7], cotton [8], agriculture crop residues [9], and bamboo [10]. LCNF have diameters ranging from a few nanometers to tens of nanometers [11,12]. They have low thermal expansion [13,14], good mechanical and optical properties [14,15], and high surface area and aspect ratios [16]. LCNF potentially have application in various fields, including composite materials [12,17,18], medicine [19,20], papermaking [21], rheology modifiers, and dispersion stabilizers [12,22].

One major drawback associated with the applications of conventional cellulose nanofibers (CNF) is their dispersion ability in non-polar media because of their hydrophilic nature [23,24]. LCNF, produced from materials containing liginin, can have better dispersion ability in non-polar media, because it can be less polar and more hydrophobic than CNF. The polarity and hydrophilicity of LCNF could be adjusted by lignin. LCNF production can also provide opportunities to reduce production costs and environmental pollution by reducing raw material, chemical, and energy requirements [23-25].

Cellulose nanofibers were first isolated from dilute slurries of cut cellulose fibers via mechanical disintegration in 1983 [17]. Thereafter, researchers have tried to isolate mostly CNF with low lignin content via mechanical disintegration [18,21,26,27]. The widely applied mechanical disintegration techniques include homogenization, super-grinding, cryocrushing, and microfluidization [28]. Homogenization uses the high shear rate within a homogenizer chamber to fibrillate the fibers in aqueous suspension [28]. In a super-grinding process, wood fibers are forced through a grinder with a static grind stone and a rotating grind stone. The contact with the grind stones and the repeated cyclic stresses lead to fibrillation of the fibers [29-31]. In a cryocrushing process, the refined fibers are frozen by liquid nitrogen and the fibrils are isolated by high impact grinding performed under the surface of the liquid nitrogen [32,33]. In microfluidization, the feedstock material is passed through an intensifier pump that can raise the pressure up to hundreds of megapascals (MPa). The fibers are defibrillated into nanofibers by shear forces provided by an interaction chamber, which can be designed with different geometries to produce different sized materials and resolve the plugging by using reverse flow [29].

In our study, we used microfluidization on the pretreated wood samples. The main issue with mechanical disintegration techniques is the high energy consumption used to convert cellulose fibers into nanoscale fibrils. The energy needed for overcoming the interfibrillar hydrogen bonding ranged between 5278 kWh/ton and 5833 kWh/ton. The energy consumption of the actual fibrillation without pretreatment could be a few times higher [3,34]. By using certain pretreatments, such as TEMPO oxidation [35-37], carboxymethylation [38-40], alkali pretreatment and enzymatic pretreatment [3,41-43], or microemulsion treatment [44], the energy consumption of mechanical disintegration can be considerably

decreased. The current energy consumption levels of CNF production have been considered to be industrially acceptable; however, there are still demands for the research and industry communities to develop more energy-efficient and sustainable routes to produce CNF or LCNF [45].

The objective of this study was to produce and evaluate LCNF from steam-exploded and partial enzymatic-hydrolyzed hardwood pulp and organosolv pretreated softwood pulp streams. Microfluidization was used as a mechanical defibrillation method in a laboratory scale production of LCNF from different streams.

Feed streams for LCNF processing

In biorefining of lignocellulosics to fuel, the narrow profit margins of bioethanol production make the smallest waste painful. The goal is to maximize the use of every stream. Biorefining lignocellulosic biomass to ethanol is an excellent platform from which to withdraw side streams and produce LCNF (**Fig. 1**). While producing ethanol, a successful bioproducts plant has to bring higher value chemicals and fibers from co-products and byproducts [46-49]. The bioconversion process, which is the backbone of cellulosic biomass refineries, constitutes three major unit operations: 1) pretreatment, 2) hydrolysis, and 3) fermentation [50]. This research focuses on a high value added co-product opportunity by drawing cellulose-rich side streams containing lignin from pretreatment and enzymatic hydrolysis stages and converting them into nanofibers by using a mechanical disintegration process.

A steam exploded and partial enzymatic hydrolyzed hardwood pulp (SEPE hardwood pulp) and an organosolv pretreated softwood pulp (OP softwood pulp) were chosen to prepare LCNF via microfluidization as a method suitable for laboratory-scale high pressure production. The reasons to develop these two routes are: 1) woody biomass is one of the most abundant biomaterials [51], and 2) organosolv pulping processes are relatively clean and compatible with the enzymatic hydrolysis and fermentation stages of biorefining, compared to other chemical methods [10,52]. Steam explosion processes are also relatively clean and only require mild chemical treatment [21,53]. The energy consumptions of these two routes for LCNF preparation were evaluated and the properties of two types of LCNF obtained: hardwood-lignocellulose nanofibers (HW-LCNF) and softwood-lignocellulose nanofibers (SW-LCNF). Their suspensions also were investigated for potential application as rheological modifiers and reinforcing agents.

MATERIALS AND METHODS

Materials

Two types of pretreated wood pulps were used to prepare LCNF: 1) SEPE hardwood pulp, and 2) OP softwood pulp.

SEPE hardwood pulp

The SEPE hardwood pulp was provided by Mascoma. The compositions of the pulp were 57% lignin (acid insoluble), 40% cellulose (glucan), 3.5% hemicellulose (pentosans), and 0.5% ash, as determined by TAPPI Standard Test Methods T 222-om11 "Acid-insoluble lignin in wood and pulp," T 201 wd-76 "Cellulose in pulp (Cross and Bevan Method)," T 223 cm-10 "Pentosans in wood and pulp," and T 244 cm-11 "Acid-insoluble ash in wood, pulp, paper, and paperboard," respectively. The component sum was slightly more than 100% because of experimental error.

OP softwood pulp

Lodgepole pine trees infested by mountain pine beetles at the gray phase and harvested at Prince George and Quesnel in British Columbia, Canada, were used as a feedstock. The average age of the trees was 99 years [54].

After being debarked and air-dried, the tree trunks were chipped and screened using a plate screen. The fractions

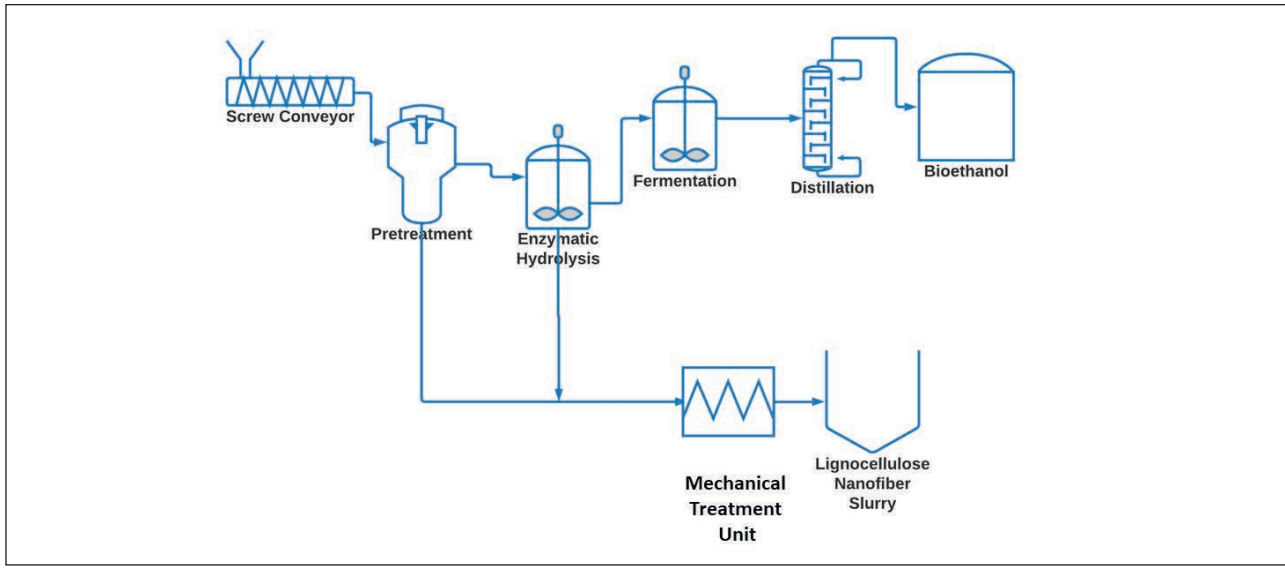

1. Flow diagram of a biorefining to ethanol and lignocellulose nanofiber (LCNF) productions.

with a size between 2.5 cm × 2.5 cm and 5.0 cm × 5.0 cm that were approximately 0.5 cm thick were collected as the feedstock for ethanol organosolv pretreatment. Chips were pulped in a 65% ethanol (a 7:1 weight ratio to wood chips) aqueous solution with sulfuric acid as a catalyst (weight ratio to wood chips, 1.1:100), using a custom-built four-vessel (2 L each) rotating digester (Aurora Products Ltd.; Savona, BC, Canada). Four batches of 200 g chips (oven dried weight) were pulped in each of the four vessels. The pretreated materials were washed with a 60°C fresh 65% ethanol aqueous solution, and then washed with 60°C water. The washed substrate was split into eight equal portions and homogenized in a standard British disintegrator for 5 min and passed through a laboratory flat screen with 0.008 in slits to remove the rejects. The amount of rejects collected was 4.2% of the feedstock. The pulp was delignified at room temperature using acidified sodium chlorite according to PAPTAC Useful Method G10.U "Chorite Delignification of Cellulose Materials" to preserve the carbohydrates. The obtained pulp contained 93% glucan, 0.8% mannan, 0.9 % xylan, 0.3% galactan, and 2% acid insoluble lignin. This composition was measured according to the method outlined by Sluiter et al. [55].

Fibrillation

The hardwood and softwood pulps were suspended in water with consistencies of 0.5 wt% and 1 wt%. All suspensions were chopped before being fed to a microfluidizer. The hardwood suspensions were chopped with high shear mixer at a rate of 10 min/500 mL. The particle size of the softwood pulp was too large; therefore, it was chopped using a Black & Decker Cyclone kitchen blender (475 watts) at speed 18 for 6 min before being chopped with a higher shear mixer at a rate of 10 min/500 mL. The fibrillation of chopped pulps was achieved by multiple passes through an M-110EH-30 microfluidizer (Microfluidics; Westwood, MA, USA). The z-shaped interaction chambers had four different diameters: 87 µm; 100 µm; 200 µm, and "blank." The "blank" here means a diameter in millimeters, which was too big to perform fibrillation. It was only used as a place holder because two chambers were required for operation.

CHARACTERIZATION OF LCNF

Conductivity measurement

The conductivity of LCNF suspensions was measured with Thermo Scientific (Beverly, MA, USA) Orion 5-Star Plus Multimeter with a Dura Probe 4-electrode cell at room temperature.

Colloidal stability

We suspended 0.125 wt% LCNF in a mixture of ethylene glycol and water with a 1:1 weight ratio. The stability of LCNF suspensions was measured with a Turbiscan LAB stability analyzer (Formulaction; Toulouse, France), which scanned a sample vial from its bottom to its top and measured the transmission data. Each sample was scanned once per minute for 1 h.

Electron microscopy

Scanning transmission electron microscopy (STEM) was used to investigate the morphologies of prepared LCNF. To prepare samples for STEM testing, a 0.1 wt% LCNF suspension in water was dropped on a carbon copper grid, which was blotted and stained with one drop of 2 wt% uranyl acetate for 5 min.

Dynamic light scattering

We used a Zetasizer Nano-ZS system (Malvern Panalytical; Malvern, UK) to determine the hydrodynamic radius of LCNF particles, which were dispersed in water with a consistency of 0.1 wt%. Measurements were made with a temperature regulated cell set at 25°C (±0.1°C).

Rheology test

The steady state rheology of LCNF suspensions in mixtures of ethylene glycol and water with a 1:1 weight ratio was measured by AR-G2 Rheometer (TA Instruments; New Castle, DE, USA) with cone and plate (1° nominal angle) geometry at 25°C. The dynamic rheology of suspensions was measured with the same geometry and settings. To determine the linear viscoelastic range, the torque sweep was measured at 1 Hz. A strain of 0.07 was chosen for the frequency sweep test of LCNF suspensions.

RESULTS AND DISCUSSION

HW-LCNF and SW-LCNF preparation

The SEPE hardwood and OP softwood pulps were diluted in water to prepare suspensions with consistencies of 0.5 and 1 wt% for fibrillation via microfluidization. The SEPE hardwood pulp could be defibrillated successfully at both consistencies. However, the OP softwood pulp was only successfully defibrillated at 0.5 wt% and its 1 wt% suspension clogged the microfluidizer. **Table I** shows details of about the optimized fibrillation processes. The SEPE hardwood pulp suspensions with very high lignin content needed seven passes through the microfluidizer, but the OP softwood pulp with less lignin only went through the microfluidizer for four times.

Previous studies have investigated the energy consumption of the fibrillation process based on a method reported by Ankerfors [45,56]. This method was developed based on the energy balance of the fibrillation process. A simplified equation was given by Ankerfors in the following form [57]:

$$\frac{1}{\rho}(p_2 - p_1) + w_{CV} = 0 \quad (1)$$

where ρ is the fluid density, p_2 is the pressure at a position right after the pressure pump that pressurized the systems, p_1 is the pressure at the surface of the inlet tank, and W_{cv} is the performed work. This equation was simplified based on the following assumptions: 1) the flowrate was constant, 2) there was no change in internal energy, 3) the suspensions were incompressible fluids, 4) the height of position 1 and 2 were equal, 5) the changes in dynamic energy could be neglected,

Pass	SEPE Hardwood Pulp/Water (0.5, 1 wt%)			OP Softwood Pulp/Water (0.5 wt%)		
	First Chamber Size, μm	Second Chamber Size, μm	Pressure, MPa	First Chamber Size, μm	Second Chamber Size, μm	Pressure, MPa
1	Blank	200	21	Blank	200	21
2	200	100	34	Blank	200	21
3	200	100	34	Blank	200	21
4	200	87	41	Blank	200	21
5	200	87	41	—	—	—
6	200	87	41	—	—	—
7	200	87	41	—	—	—

I. Process conditions and observations of the fibrillation of the wood pulps (SEPE = steam exploded and partial enzymatic hydrolyzed; OP = organosolv pretreated).

			Energy Consumption, kWh/ton	
			HW-LCNF	SW-LCNF
Each Pass	1st	5.8	5.8	
	2nd	9.5	5.8	
	3rd	9.5	5.8	
	4th	11.4	5.8	
	5th	11.4	—	
	6th	11.4	—	
	7th	11.4	—	
Total	0.5 wt%	wet basis	70.4	23.2
		dry basis	14080	4640
	1 wt%	wet basis	70.4	—
		dry basis	7040	—

II. Energy consumption of fibrillation process via microfluidization (HW-LCNF = hardwood-lignocellulose nanofibers; SW-LCNF = softwood lignocellulose nanofibers).

and 6) the heat due to frictions could be neglected. This equation could be used to estimate the energy consumption of each pass. The total energy consumption of fibrillation via microfluidization would be the sum of the energy consumption of each pass.

Table II lists the calculated values of the energy consumptions of the preparations of HW-LCNF and SW-LCNF in this research. The value of wet basis was the energy consumption per metric tons of the mixture of LCNF (0.5 wt% and 1 wt%) and water. The value of dry basis was calculated based on the yield of dried materials. Because SW-LCNF required lower operating pressure and fewer passes of fluids through the fluidizer than did the HW-LCNF, the production of SW-LCNF used much less energy than did the production of HW-LCNF. Table II also shows that there was a significant decrease of consumed energy when 1 wt% SEPE hardwood pulp was fed into the fibrillation process. This indicated that the energy consumption of LCNF production via microfluidization could be optimized by adjusting the consistency of feeding fluid, as long as the material does not block the fluidizer.

To better understand the fibrillation processes via microfluidization for these two LCNF preparation routes, we compared the values of the energy consumptions of fibrillation with the consumed energy for the CNF fibrillation process via microfluidization reported by other researchers (**Table III**) [29,40,56,57]. The reported values are the fibrillation energy consumption of microfluidization processes without considering the cost in other stages, such as pretreatment. Consistencies of defibrillated fiber slurries were comparable. As expected, Table III shows that organosolv pretreated SW-LCNF production used much less energy than did the steam explosion and partially enzymatic treated HW-LCNF. SW-LCNF production used much less energy than did HW-LCNF. The energy costs of fibrillation processes of these two LCNF production routes were higher than the values of CNF production reported by Spence et al. [29], Taiple et al. [40], and An-

No.	Source Materials	Pretreatment	Energy Consumption, Dried Material	Reference
1	Hardwood pulp	Steam explosion and partially enzymatic treated	7040–14080	This research
2	Softwood pulp	Organosolv pretreated	4640 kWh/ton	This research
3	Various never dried and once dried pulps: bleached softwood sulfite pulp, kraft pulp	Carboxymethylation; carboxymethyl cellulose (CMC) modification; enzymatic and mechanical	27000 kWh/ton without pretreatment; 500–2300 kWh/ton with pretreatment	[57]
4	Elemental chlorine free bleached hardwood kraft pulp	Carboxymethylation	5500 kWh/ton per pass without pretreatment; 2200 kWh/ton per pass with pretreatment	[40]
5	Never-dried bleached and unbleached kraft hardwood pulps	Mechanically refined in a Valley beater	2286–3119 kWh/ton, varied according to the number of passes and operating pressures	[29]
6	Never-dried totally chlorine-free bleached sulfite dissolving pulp from a mixture of spruce (60%) and pine (40%)	Carboxymethyl cellulose (CMC) modification	2700–181500 kWh/ton, varied according to the number of passes and the dry content of suspensions	[56]

III. Comparison of the energy consumption for the fibrillation processes with reported works via microfluidization.

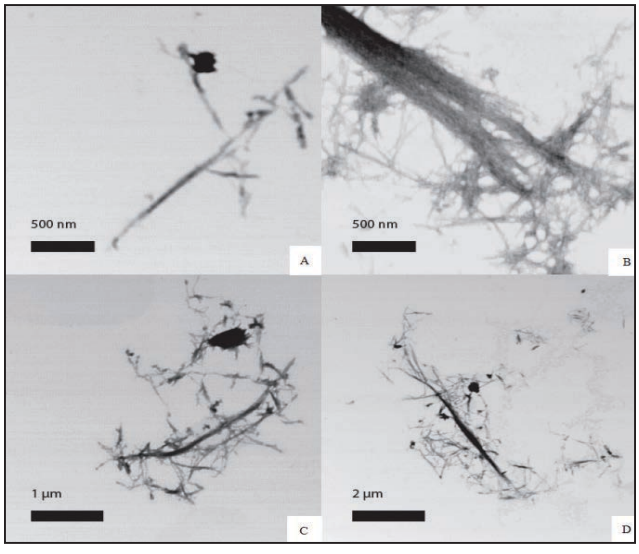

2. Typical canning transmission electron micrographs of hardwood-lignocellulose nanofibers (HW-LCNF).

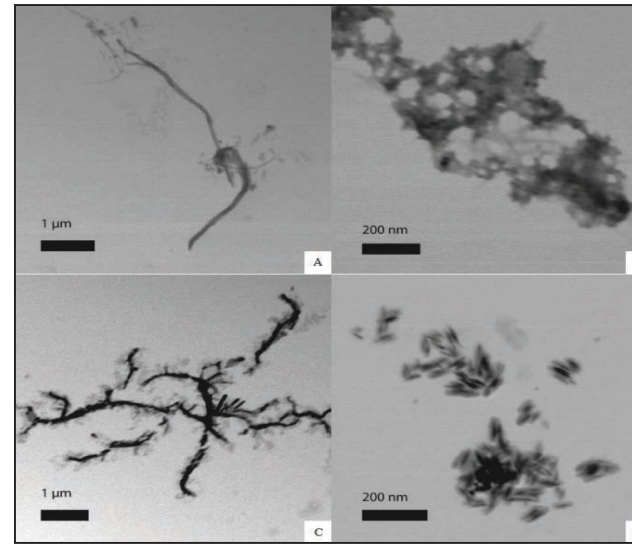

3. Typical scanning transmission electron micrographs of softwood-lignocellulose nanofibers (SW-LCNF).

kerfors [57], but lower than reported by Naderi [56]. As reported in those studies, carboxymethylation of pulp greatly enhances microfibrillation.

Properties of HW-LCNF, SW-LCNF, and their suspensions

The properties of LCNF, including morphology, geometry, crystallinity, specific surface area, stability, conductivity, and rheological behavior of their suspensions, are important for their applications. This section focuses on the investigation of the morphology and dimensions of the fibrils and the colloidal stability, conductivity, and rheological behaviors of their suspensions, which are critical information for their potential applications as rheological modifiers and reinforcing agents.

Morphology and dimension of HW-LCNF and SW-LCNF

The morphology of both types of LCNF was observed using STEM to investigate the homogeneity of samples and deter-

mine the diameters of fibrils. The significant differences between the preparation conditions of HW-LCNF and SW-LCNF implied that the morphologies and dimensions of these two types of LCNF would be significantly different. **Figures 2 and 3** show typical STEM micrographs of these two types of LCNF. HW-LCNF had fibrils with and without branches (Figs. 2A, 2C, and 2D) and fibril bundles (Fig. 2B). The presence of residual fibril bundles was probably the result of incomplete fibrillation, which was also noted by other researchers [10,25]. As a result of the existence of fibril bundles (Fig. 2), the average diameter of hardwood fibrils was about 345 nm, which was determined from 33 STEM micrographs. This value is much higher than the typical values of nanofibers (a few nanometers to tens of nanometers) reported by other researchers [11,12], indicating that the percentage of nanofibers in the final products was relatively low and the amount of fibril bundles was higher. The morphologies of the LCNF made from softwood pulp were more diversified, including typical fibril (Fig. 3A), star fish-like shape (Fig. 3C), agglomerated particles (Fig. 3D), and an irregular shape (Fig. 3B). The diversity of shapes made it impossible to obtain an accurate average diameter of SW-LCNF from the STEM images. Figures 2 and 3 also show that the length of fibrils was in the range of several microns, which was the typical range of the length of cellulose nanofibers.

Colloidal stability of suspensions

The conductivity of individual HW-LCNF and SW-LCNF suspensions were 4.2 μS/cm and 7.9 μS/cm, respectively. Suspensions with such low conductivities could be treated as nonionic. Therefore, although the electrochemical properties of nanofibers might affect the dispersion, aggregation, and rheological properties of their suspensions [58,59], their potential influence is not discussed here.

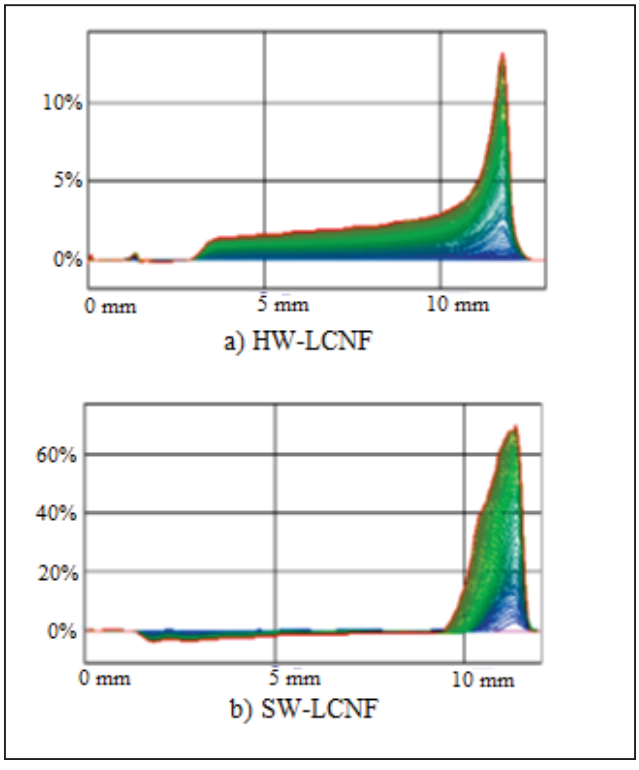

4. Light transmission data for 0.125 wt% HW-LCNF and SW-LCNF suspensions at consistencies of a) 0.125 wt% and b) 0.25 wt%.

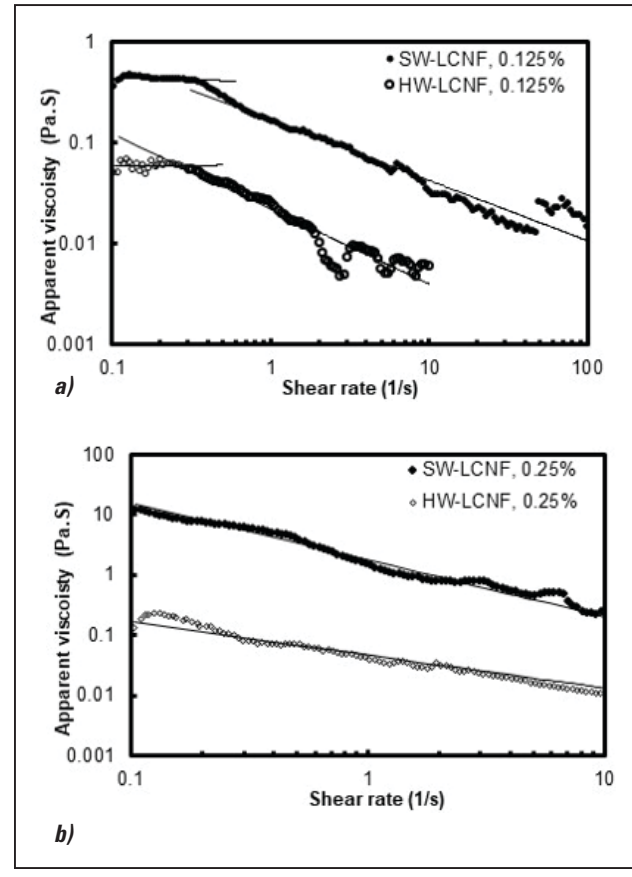

5. Apparent viscosities of lignocellulose nanofiber suspensions as a function of shear rate.

The dispersions of HW-LCNF and SW-LCNF in mixtures of ethylene glycol and water with a 1:1 weight ratio were evaluated by testing 0.125 wt% suspensions. **Figure 4** shows the delta transmission data of light. The x-axes in Figs. 4a and 4b reflect the heights of sample vials, with the left ends of x-axes representing bottoms and the right ends of x-axes representing tops. Both vials were filled to 14 mm. For the HW-LCNF suspension, the delta transmission data gradually increased from the vial's bottom to the middle and increased about 15% at the vial's top in an hour, as the amount of time advanced from the bluish to reddish lines. However, for the SW-LCNF suspensions, the increase of the delta transmission was only detected at the vial's top, and was quite significant. It reached more than 60% in an hour. The changes in the delta transmission of light indicated the aggregation and sedimentation of fibrils. However, the sedimentation only happened at the bottom of the vial containing an HW-LCNF suspension. This might result from the high percentage of fibril bundles in the suspension.

Rheological behavior of suspensions

The steady state behavior of suspensions versus shear rate could be influenced by the consistency of suspensions and the dimension/flexibility of nanofibers. For the suspensions with same types of CNF, their viscosities increase with the increase of consistency because of the formation of more rigid fibril networks [59,60]. For the suspensions with same consistencies, the CNF suspensions could become more viscous when the aspect ratio of CNF increases and the fibrils become more flexible [61].

The shear thinning behavior and secondary shear-thickening behavior of CNF suspensions have been reported in previous studies [28,42,60,62,63]. **Figure 5** shows the shear rate dependences of the apparent viscosities of HW-LCNF and SW-LCNF suspensions. When the consistencies of suspensions were same, the apparent viscosities of SW-LCNF suspension were higher than the apparent viscosities of the HW-LCNF suspension at the same shear rate. However, the shear rate dependences of the viscosities of LCNF suspensions were quite different at the investigated consistencies. As seen in Fig. 5a, the HW-LCNF and SW-LCNF suspensions with 0.125 wt% consistency showed Carreau fluid rheology behavior: Newtonian plateau regions at the very low shear rate range (<0.3 s^{-1}) and shear thinning regions at the higher shear rate range (>0.3 s^{-1}). This flow behavior can be described by Carreau's model [64,65]:

$$\eta - \eta_\infty = \frac{\eta_0 - \eta_\infty}{[1+(\lambda\dot{\gamma})^2]^{m/2}} \quad (2)$$

where $\dot{\gamma}$ is the shear rate; η is the apparent viscosity; η_0 and η_∞ are viscosities at zero shear rate and infinite shear rate, respectively; λ is Carreau's model characteristic time constant; and m is the dimensionless rate constant, whose negative value shows the slope of the viscosity versus the shear rate in the shear-thinning region. The η_0 values of HW-LCNF and SW-LCNF suspensions could be obtained from Eq. 2 by simulation or from the average value of the data of the Newtonian plateau region. As Fig. 4a shows, the η_0 value (0.425 Pa·S) of 0.125 wt% SW-LCNF suspension was much higher than the η_0 value (0.058 Pa·S) of 0.125 wt% HW-LCNF suspension. Generally, the HW-LCNF and SW-LCNF suspensions with higher solid contents (0.25 wt%) showed shear thinning behaviors (Fig. 4b), which were usually the results of the disentanglement or break-down of fibril networks. However, the 0.25 wt% HW-LCNF suspension showed a shear thickening behavior at the early beginning of the tested shear rate range. This minor shear thickening phenomenon might result from the flow-induced stretching of fibrils or unpacking of fibril bundles [28].

The viscosity fluctuations of all suspensions also could be seen in the shear thinning regions, and the viscosity fluctuations of HW-LCNF were more obvious. This might be the result of the stretching and unpacking of fibril bundles under the influence of shear stress, which agrees with the inhomogeneous morphology illustrated by the STEM micrographs.

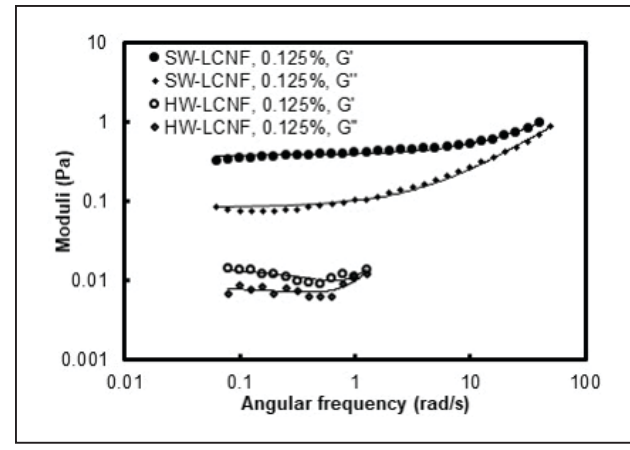

6. Storage and loss moduli of lignocellulose nanofiber suspensions as a function of angular frequency.

The suspensions' fibril network structures could also be examined by dynamic rheology test. **Figure 6** shows the frequency sweep plots of HW-LCNF and SW-LCNF suspensions. The storage modulus G' and the loss modulus G'' of the SW-LCNF suspension were much higher than the moduli of the HW-LCNF suspension. This indicates a stronger network of SW-LCNF, which is in agreement with the steady state test. Although the consistency of the suspensions was quite low, both suspensions displayed gel-like behavior: 1) the G' values of both suspensions were independent of the angular frequency in most of the tested frequency ranges; 2) the G'' values didn't change very much when the angular frequency was low; and 3) the G'' values were less than the G' values. This gel-like behavior of LCNF suspensions at a very low consistency indicated that it is very easy for HW-LCNF and SW-LCNF to form strong physical entanglements between fibrils because of their large aspect ratio and high flexibility [60].

CONCLUSION

We investigated two types of LCNF to develop routes for energy-efficient and sustainable LCNF production. These included a steam-exploded and partial enzymatic hydrolyzed hardwood pulp (HW-LCNF) and an organosolv pretreated softwood pulp via microfluidization (SW-LCNF) The energy consumptions of the fibrillation processes of the HW-LCNF and the SW-LCNF productions were about 7040–14,080 kWh/ton and 4640 kWh/ton, respectively. In comparison with steam explosion and partial enzymatic treatment, organosolv pulping greatly enhances defibrillation.

The HW-LCNF had fibril shapes with and without branches and bundle shape. Bundles reduced the colloidal stabilities of its suspensions and weakened the strength of its fibril networks in suspensions. The SW-LCNF had more diversified morphologies, including fibril shape, starfish-like shape, irregular shape, and agglomerated particles. Its suspensions had better colloidal stabilities and stronger fibril networks. The

shear rate dependence of the apparent viscosities of HW-LCNF and SW-LCNF suspensions could be affected by the LCNF consistency. Their 0.125 wt% suspensions acted like Carreau fluids and their 0.25 wt% suspensions showed near shear-thinning behavior. When the consistency was the same, the SW-LCNF suspension had higher zero shear rate viscosity (η_0) and higher apparent viscosities than did the HW-LCNF suspension. **TJ**

ACKNOWLEDGMENTS

We thank NSERC Bioconversion Network – Grant NETGP 350246 for providing the funding and Alberta Innovates Technology Futures (AITF) for providing high shear mixer and microfluidizer; Frank Tosto for assistance with equipment operation at AITF; National Institute of Nanotechnology for providing characterization facilities; and Mascoma Romeo's cake feedstock pulp.

LITERATURE CITED

1. Chen, W., Yu, H., Liu, Y., et al., *Carbohydr. Polym.* 83(4): 1804(2011). https://doi.org/10.1016/j.carbpol.2010.10.040.
2. Sacui, I.A., Nieuwendaal, R.C., Burnett, D.J., et al., *ACS Appl. Mater. Interfaces* 6(9): 6127(2014). https://doi.org/10.1021/am500359f.
3. Zhu, J.Y., Sabo, R., and Luo, X., *Green Chem.* 13(5): 1339(2011). https://doi.org/10.1039/c1gc15103g.
4. Liimatainen, H., Visanko, M., Sirviö, J., et al., *Cellulose* 20(2): 741(2013). https://doi.org/10.1007/s10570-013-9865-y.
5. Liimatainen, H., Visanko, M., Sirviö, J.A., et al., *Biomacromolecules* 13(5): 1592(2012).
6. Kaushik, A. and Singh, M., *Carbohydr. Res.* 346(1): 76(2011). https://doi.org/10.1016/j.carres.2010.10.020.
7. Hrabalova, M., Schwanninger, M., Wimmer, R., et al., *BioResources* 6(2): 1631(2011).
8. de Morais Teixeira, E., Corrêa, A.C., Manzoli, A., et al., *Cellulose* 17(3): 595(2010). https://doi.org/10.1007/s10570-010-9403-0.
9. Chaker, A., Mutjé, P., Vilar, M.R., et al., *Cellulose* 21(6): 4247(2014). https://doi.org/10.1007/s10570-014-0454-5.
10. da Costa Correia, V., dos Santos, V., Sain, M., et al., *Cellulose* 23(5): 2971(2016). https://doi.org/10.1007/s10570-016-0996-9.
11. Lavoine, N., Desloges, I., Dufresne, A., et al., *Carbohydr. Polym.* 90(2): 735(2012). https://doi.org/10.1016/j.carbpol.2012.05.026.
12. Lindstrom, T., Naderi, A., and Wiberg, A., *J. Korea Tech. Assoc. Pulp. Pap. Ind.* 47(6): 5(2015).
13. Fukuzumi, H., Saito, T., Iwata, T., et al., *Biomacromolecules* 10(1): 162(2008). https://doi.org/10.1021/bm801065u.
14. Iwamoto, S., Nakagaito, A., and Yano, H., *Appl. Phys. A* 89(2): 461(2007). https://doi.org/10.1007/s00339-007-4175-6.
15. Rodionova, G., Lenes, M., Eriksen, Ø., et al., *Cellulose* 18(1): 127(2011). https://doi.org/10.1007/s10570-010-9474-y.
16. Moon, R.J., Martini, A., Nairn, J., et al., *Chem. Soc. Rev.* 40(7): 3941(2011). https://doi.org/10.1039/c0cs00108b.
17. Khalil, H.A., Bhat, A., and Yusra, A.I., *Carbohydr. Polym.* 87(2): 963(2012). https://doi.org/10.1016/j.carbpol.2011.08.078.
18. Siró, I. and Plackett, D., *Cellulose* 17(3): 459(2010). https://doi.org/10.1007/s10570-010-9405-y.
19. Cai, H., Sharma, S., Liu, W., et al., *Biomacromolecules* 15(7): 2540(2014). https://doi.org/10.1021/bm5003976.
20. Bhattacharya, M., Malinen, M.M., Lauren, P., et al., *J. Controlled Release* 164(3): 291(2012). https://doi.org/10.1016/j.jconrel.2012.06.039.
21. Osong, S.H., Norgren, S., and Engstrand, P., *Cellulose* 23(1): 93(2016). https://doi.org/10.1007/s10570-015-0798-5.
22. Andresen, M. and Stenius, P., *J. Dispersion Sci. Technol.* 28(6): 837(2007). https://doi.org/10.1080/01932690701341827.
23. Spence, K.L., Venditti, R.A., Habibi, Y., et al., *Bioresour. Technol.* 101(15): 5961(2010). https://doi.org/10.1016/j.biortech.2010.02.104.
24. Rojo, E., Peresin, M.S., Sampson, W.W., et al., *Green Chem.* 17(3): 1853(2015). https://doi.org/10.1039/C4GC02398F
25. Spence, K.L., Venditti, R.A., Rojas, O.J., et al., *Cellulose* 17(4): 835(2010). https://doi.org/10.1007/s10570-010-9424-8.
26. Klemm, D., Kramer, F., Moritz, S., et al., *Angew. Chem. Int. Ed.* 50(24): 5438(2011). https://doi.org/10.1002/anie.201001273.
27. Hoeger, I.C., Nair, S.S., Ragauskas, A.J., et al., *Cellulose* 20(2): 807(2013). https://doi.org/10.1007/s10570-013-9867-9.
28. Taheri, H. and Samyn, P., *Cellulose* 23(2): 1221(2016). https://doi.org/10.1007/s10570-016-0866-5.
29. Spence, K.L., Venditti, R.A., Rojas, O.J., et al., *Cellulose* 18(4): 1097(2011). https://doi.org/10.1007/s10570-011-9533-z.
30. Abe, K., Iwamoto, S., and Yano, H., *Biomacromolecules* 8(10): 3276(2007). https://doi.org/10.1021/bm700624p.
31. Iwamoto, S., Nakagaito, A., Yano, H., et al., *Appl. Phys. A* 81(6): 1109(2005). https://doi.org/10.1007/s00339-005-3316-z.
32. Chakraborty, A., Sain, M., and Kortschot, M., *Holzforschung* 59(1): 102(2005). https://doi.org/10.1515/HF.2005.016.
33. Janardhnan, S. and Sain, M.M., *BioResources* 1(2): 176(2007).
34. Bharimalla, A.K., Deshmukh, S.P., Patil, P.G., et al., *World J. Nano Sci. Eng.* 5(04): 204(2015). https://doi.org/10.4236/wjnse.2015.54021.
35. Shinoda, R., Saito, T., Okita, Y., et al., *Biomacromolecules* 13(3): 842(2012). https://doi.org/10.1021/bm2017542.
36. Milanovic, J., Kostic, M., Milanovic, P., et al., *Ind. Eng. Chem. Res.* 51(29): 9750(2012). https://doi.org/10.1021/ie300713x.
37. Gamelas, J.A., Pedrosa, J., Lourenço, A.F., et al., *Micron* 72: 28(2015). https://doi.org/10.1016/j.micron.2015.02.003.
39. Siró, I., Plackett, D., Hedenqvist, M., et al., *J. Appl. Polym. Sci.* 119(5): 2652(2011). https://doi.org/10.1002/app.32831.
40. Taipale, T., Österberg, M., Nykänen, A., et al., *Cellulose* 17(5): 1005(2010). https://doi.org/10.1007/s10570-010-9431-9.
41. Wang, Q., Wei, W., Chang, F., et al., *BioResources* 11(1): 2536(2016).
42. Pääkkö, M., Ankerfors, M., Kosonen, H., et al., *Biomacromolecules* 8(6): 1934(2007). https://doi.org/10.1021/bm061215p.
43. Bhattacharya, D., Germinario, L.T., and Winter, W.T., *Carbohydr. Polym.* 73(3): 371(2008). https://doi.org/10.1016/j.carbpol.2007.12.005.
44. Carrillo, C.A., Laine, J., and Rojas, O.J., *ACS Appl. Mater. Interfaces* 6(24): 22622(2014). https://doi.org/10.1021/am5067332.
45. Naderi, A., Lindström, T., and Sundström, J., *Cellulose* 22(2): 1147(2015). https://doi.org/10.1007/s10570-015-0576-4.

46. Nakagame, S., Chandra, R.P., Kadla, J.F., et al., *Biotechnol. Bioeng.* 108(3): 538(2011). https://doi.org/10.1002/bit.22981.
47. Nakagame, S., Chandra, R.P., and Saddler, J.N., *Biotechnol. Bioeng.* 105(5): 871(2010). https://doi.org/10.1002/bit.22626.
48. Sims, R.E., Mabee, W., Saddler, J.N., et al., *Bioresour. Technol.* 101(6): 1570(2010). https://doi.org/10.1016/j.biortech.2009.11.046.
49. Kumagai, A., Lee, S.H., and Endo, T., *Biotechnol. Bioeng.* 113(7): 1441(2016). https://doi.org/10.1002/bit.25911.
50. Pan, X., Xie, D., Yu, R.W., et al., *Ind. Eng. Chem. Res.* 46(8): 2609(2007). https://doi.org/10.1021/ie061576l.
51. Moon, D., Yagishita, T., Minowa, T., et al., *Trans. ASABE* 56(3): 1061(2013).
52. Pan, X., Arato, C., Gilkes, N., et al., *Biotechnol. Bioeng.* 90(4): 473(2005). https://doi.org/10.1002/bit.20453.
53. Kumar, L., Chandra, R., and Saddler, J., *Biotechnol. Bioeng.* 108(10): 2300(2011). https://doi.org/10.1002/bit.23185.
54. Pan, X., Xie, D., Yu, R.W., et al., *Biotechnol. Bioeng.* 101(1): 39(2008). https://doi.org/10.1002/bit.21883.
55. Sluiter, A., Hames, B., Ruiz, R., et al., "Determination of structural carbohydrates and lignin in biomass," Laboratory Analytical Procedure, NREL Technical Report NREL/TP-510-42618, U.S. Department of Energy, April 2008 (Rev. 08-03-2012).
56. Naderi, A., Lindström, T., Sundström, J., et al., *Cellulose* 22(2): 1159(2015). https://doi.org/10.1007/s10570-015-0577-3.
57. Ankerfors, M., "Microfibrillated cellulose: energy-efficient preparation techniques and applications in paper," Doctoral thesis, KTH Royal Institute of Technology, Stockholm, Sweden, 2015.
58. Sim, K., Lee, J., Lee, H., et al., *Cellulose* 22(6): 3689(2015). https://doi.org/10.1007/s10570-015-0784-y.
59. Jowkarderis, L. and van de Ven, T.G., *Cellulose* 21(4): 2511(2014). https://doi.org/10.1007/s10570-014-0292-5.

ABOUT THIS PAPER

Cite this article as:
Sun C., Gao, Y., Chandra, R., and Boluk, Y., *TAPPI J.* 18(4): 233(2019). https://doi.org/10.32964/TJ18.4.233

DOI: https://doi.org/10.32964/TJ18.4.233

ISSN: 0734-1415

Publisher: TAPPI Press

60. Li, M.-C., Wu, Q., Song, K., et al., *ACS Sustainable Chem. Eng.* 3(5): 821(2015). https://doi.org/10.1021/acssuschemeng.5b00144.
61. Tanaka, R., Saito, T., Hondo, H., et al., *Biomacromolecules* 16(7): 2127(2015). https://doi.org/10.1021/acs.biomac.5b00539.
62. Butchosa, N. and Zhou, Q., *Cellulose* 21(6): 4349(2014). https://doi.org/10.1007/s10570-014-0452-7.
63. Colson, J., Bauer, W., Mayr, M., et al., *Cellulose* 23(4): 2439(2016). https://doi.org/10.1007/s10570-016-0987-x.
64. Carreau, P., Kee, D.D., and Daroux, M., *Can. J. Chem. Eng.* 57(2): 135(1979). https://doi.org/10.1002/cjce.5450570202.
65. Machač, I., Šiška, B., and Machačová, L., *Chem. Eng. Process.: Process Intensification* 39(4): 365(2000). https://doi.org/10.1016/S0255-2701(99)00101-4.

ABOUT THE AUTHORS

We conducted this research because of our interest in the manufacture of high value-added cellulose products. All of my (Boluk's) research has been on nanocelluloses, which include cellulose nanocrystals and cellulose nanofibers.

The most difficult part of this work has been to minimize the energy input for lignocellulose nanofiber production. We addressed it by controlling the treatment during the biorefinery stage. A benefit to mills is the possible conversion of sidestreams to nanocellulose production.

An interesting discovery from this research is the potential for high-volume applications in cement composites. Our future research will focus on such applications.


Sun

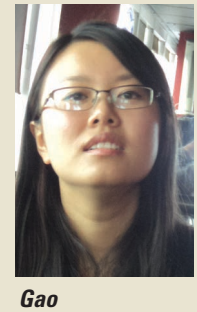
Gao


Chandra


Boluk

Sun is post-doctoral research fellow, Gao is graduate student, and Boluk is professor, Department of Civil and Environmental Engineering, University of Alberta, Edmonton, AB, Canada. Boluk is also senior research officer, National Institute for Nanotechnology, National Research Council of Canada, Edmonton. Chandra is research associate, Department of Wood Science, University of British Columbia, Vancouver, BC, Canada. Email Boluk at yaman.boluk@ualberta.ca.